A major purpose of the Technical Information Center is to provide the broadest dissemination possible of information contained in DOE's Research and Development Reports to business, industry, the academic community, and federal, state and local governments.

Although portions of this report are not reproducible, it is being made available in microfiche to facilitate the availability of those parts of the document which are legible.

LA-UR 86 4389

LA-UR--86-4389

DE87 005943

Los Alamos National Laboratory is operated by the University of California for the United States Department of Energy under contract W-7405-ENG-36

TITLE COMPUTATIONAL METHODS OF THE ADVANCED FLUID DYNAMICS MODEL

AUTHOR(S) W. R. Bohl, D. Wilhelm, F. R. Parker, J. Berthier, P. J. Maudlin, P. Schmuck, L. Goutagny, S. Ichikawa, H. Ninokata, and L. B. Luck

SUBMITTED TO ANS International Meeting on Advances in Reactor Physics, Mathematics, and Computation, Paris, France, April 27-30, 1987

## DISCLAIMER



Los Alamos Los Alamos National Laboratory
Los Alamos, New Mexico 87545

# COMPUTATIONAL METHODS OF THE ADVANCED FLUID DYNAMICS MODEL

W. R. Bohl* [Phone: (505) 667-2280]; D. Wilhelm** [Phone: (07247) 822469], F. R. Parker* [Phone: (505) 667-3177]; J. Berthier† (Phone: 11 33 42 25 7037), P. J. Maudlin* [Phone: (505) 667-3092]; P. Schmuck** [Phone: (07247) 822437], L. Goutagny† (Phone: 11 33 42 25 7057); S. Ichikawa, FACOM Division, FACOM-HITAC LTD. Sanbancho Yayoikan, 6-2, Sanban-cho Chiyoda-ku, Tokyo 102, Japan [Phone: Tokyo (03) 264-1131]; H. Hinokata, Oarai Engineering Center, Power Reactor and Nuclear Fuel Development Corporation, Oarai, Ibaraki 311-13, Japan (Phone: 0292-67-4141), and L. B. Luck* [Phone: (505) 667-3150]

## ABSTRACT

To more accurately treat severe accidents in fast reactors, a program has been set up to investigate new computational models and approaches. The product of this effort is a computer code, the Advanced Fluid Dynamics Model (AFDM). This paper describes some of the basic features of the numerical algorithm used in AFDM. Aspects receiving particular emphasis are the fractional-step method of time integration, the semi-implicit pressure iteration, the virtual mass inertial terms, the use of three velocity fields, higher order differencing, convection of interfacial area with source and sink terms, multicomponent diffusion processes in heat and mass transfer, the SESAME equation of state, and vectorized programming. A calculated comparison with an isothermal tetralin/ammonia experiment is performed. We conclude that significant improvements are possible in reliably calculating the progression of severe accidents with further development.

## I. INTRODUCTION

The analysis of hypothetical core-disruptive accidents (HCDAs) in liquid metal fast-breeder reactors (LMFBRs) involves many simplifying assumptions. At the Los Alamos National Laboratory, an international team is working to develop techniques that will allow the removal of some approximations and a reduction in the level of uncertainty. These techniques are being implemented in a computer code called the Advanced Fluid Dynamics Model (AFDM). Thus, the AFDM provides a prototype for testing algorithms leading to an improved HCDA computational capability. This paper will describe the methods currently being implemented in AFDM.

We first describe the scope of the AFDM code, including the conservation equations and the phenomenology treated. Second, the overall AFDM algorithm is presented. Third, a discussion is provided on some of the major computational features being investigated in the AFDM program. Appropriate sample calculations have been included to demonstrate the effect of differing assumptions. Finally, the current status of the AFDM code is discussed in the context of a final calculation.

## II. AFDM SCOPE

AFDM may be categorized as a three-velocity-field, two-dimensional, multiphase, Eulerian fluid-dynamics code. There are seven density components: structure, fuel

*Los Alamos National Laboratory, Q-6, MS-K557, Los Alamos, New Mexico 87545, USA
**Kernforschungszentrum Karlsruhe, Institut für Neutronenphysik and Reaktortechnik, Postfach 3640, D7500 Karlsruhe 1, Federal Republic of Germany
†Institut de Protection et de Sureté Nucléaire, CEA Cadarache, 13108, Saint-Paul-Lez-Durance, Cedex, France.

particles, fuel liquid, a coolant liquid, fuel vapor, coolant vapor, and a noncondensible gas. The fuel particles and liquid occupy one velocity field, the liquid coolant occupies a second velocity field, and the vapor species are assigned to the third velocity field. The structure field does influence both axial and radial motion; however, phenomenological modeling has concentrated on pool-type situations rather than flow channel or subassembly geometry. The structure is assumed to be stationary, and the structure volume fractions are independent of time. The conservation equations solved by AFDM are given by

$$\frac{\partial \bar{\rho}_m}{\partial t} + \nabla\cdot(\bar{\rho}_m \vec{v}_q) = -\Gamma_m \quad . \tag{1}$$

$$\frac{\partial(\bar{\rho}_q \vec{v}_q)}{\partial t} + \nabla\cdot(\bar{\rho}_q \vec{v}_q \vec{v}_q) + \alpha_q \nabla p - \bar{\rho}_q \vec{g} + K_{qS}\vec{v}_q - \sum_{q'} K_{q'q}(\vec{v}_{q'} - \vec{v}_q) - VM_q$$

$$= \sum_{q'} [\Gamma_{q'q}\vec{v}_{q'} - \Gamma_{qq'}\vec{v}_q] \quad . \tag{2}$$

$$\frac{\partial(\bar{\rho}_S e_S)}{\partial t} = Q_S \quad . \tag{3}$$

$$\frac{\partial(\bar{\rho}_p e_p)}{\partial t} + \nabla\cdot(\bar{\rho}_p e_p \vec{v}_{L1}) + p\left[\frac{\partial \alpha_p}{\partial t} + \nabla\cdot(\alpha_p \vec{v}_{L1})\right]$$

$$= Q_p + \Gamma_{L1p}\left[H(\Gamma_{L1p})e_{Sol,L1} + H(-\Gamma_{L1p})e_p\right] \quad . \tag{4}$$

$$\frac{\partial(\bar{\rho}_{L1} e_{L1})}{\partial t} + \nabla\cdot(\bar{\rho}_{L1} e_{L1} \vec{v}_{L1}) + p\left[\frac{\partial \alpha_{L1}}{\partial t} + \nabla\cdot(\alpha_{L1}\vec{v}_{L1})\right]$$

$$= Q_{L1} + \Gamma_{GL1}\left[H(\Gamma_{GL1})e_{Con,L1} + H(-\Gamma_{GL1})e_{L1}\right]$$

$$+ \Gamma_{L1p}\left[H(\Gamma_{L1p})e_{L1} + H(-\Gamma_{L1p})e_{Liq,L1}\right] \quad . \tag{5}$$

$$\frac{\partial(\bar{\rho}_{L2} e_{L2})}{\partial t} + \nabla\cdot(\bar{\rho}_{L2} e_{L2} \vec{v}_{L2}) + p\left[\frac{\partial \alpha_{L2}}{\partial t} + \nabla\cdot(\alpha_{L2}\vec{v}_{L2})\right]$$

$$= Q_{L2} + \Gamma_{GL2}\left[H(\Gamma_{GL2})e_{Con,L2} + H(-\Gamma_{GL2})e_{L2}\right] \quad , \text{ and} \tag{6}$$

$$\frac{\partial(\bar{\rho}_G e_G)}{\partial t} + \nabla\cdot(\bar{\rho}_G e_G \vec{v}_G) + p\left[\frac{\partial \alpha_G}{\partial t} + \nabla\cdot(\alpha_G \vec{v}_G)\right]$$

$$= Q_G - \sum_{i=1}^{2} \Gamma_{GLi}\left[H(\Gamma_{GLi})e_{Gi} + H(-\Gamma_{GLi})[e_{Con,Li} + \Delta h_{Li}]\right] \quad . \tag{7}$$

In these equations, $\bar{\rho}$ is a smear density, $\vec{v}$ is a velocity, p is the pressure, e is an internal energy, $\alpha$ is a volume fraction, and $\Delta h$ is the enthalpy of vaporization. The Heaviside unit function is denoted by H. The transfer rates are given by $\Gamma$ for mass, K for momentum, and Q for energy. Energy transfer includes nuclear heating. The VM term represents the virtual mass contribution. The subscripts are m for density components, q and q' for momentum components, S for structure, p for particles, L1 for fuel, L2 for coolant, G for vapor, Sol for the solidus energy, Liq for the liquidus energy, and i for an energy component summation index. Although the proper representation of the multiphase conservation equations is still controversial, the

subject of this paper is not the derivation and justification of Eqs. (1)-(7) but rather the solution algorithm and the constitutive relationships used.

## III. AFDM ALGORITHM

The AFDM is designed to use a fractional-step method for time integration in which the intracell configuration changes and the heat/mass transfers are evaluated separately from intercell convection. This type of approach has worked satisfactorily in previous multiphase codes[1,2] and significantly increases the feasibility of treating the large number of components that may be considered in HCDA analysis. A staggered finite-difference computational mesh is used, with densities, internal energies, and pressures evaluated at cell centers and velocities evaluated at the cell edges. The AFDM algorithm has four steps. These are performed sequentially without iteration in the algorithm as developed to date.

### A. Step 1. Perform Intracell Transfers

This step updates Eqs. (1)-(7) while ignoring convection. The terms treated are the partial derivatives with respect to time (or the first term in each equation) and the mass-energy transfer terms (or the right side of each equation). As explained further in Sec. IV.D, the AFDM intracell transfers are based on 12 different configurational models called topologies that describe what contacts are possible. The path through Step 1 has eight parts as follows.

1. Evaluate the equation of state (EOS).
2. Select the continuous phase and topology.
3. Calculate the source term for interfacial area changes.
4. Define flow regimes and instantaneous interfacial areas. Note that a given topology may possess more than one flow regime.
5. Perform heat and mass transfer operations.
6. Modify interfacial areas for convection based on mass transfer results.
7. Compute the momentum exchange coefficients.
8. Update velocities based on mass transfer results.

The algorithm for Step 1 is to treat rapidly varying (sensitive) quantities implicitly and the slowly varying (stable) quantities explicitly. The implicit part is treated using a multivariate Newton-Raphson algorithm. At the conclusion of Step 1, $\bar{\rho}$, $\vec{v}$, and $e$ all have been updated from intracell heat and mass transfers.

### B. Step 2. Initialize Variables for the Pressure Iteration

This step is an integration of Eqs. (1)-(7) with the right sides set to zero and the convective terms treated explicitly. The objective is to initialize the pressure iteration (Step 3) with end-of-time-step estimates for all the field variables. The mass conservation and energy conservation equations solved are

$$\bar{\rho}_{m,ij}^{n+1} = \bar{\rho}_{m,ij}^{n} - \Delta t\{[< \bar{\rho}_m^n v_q^n >_{\theta+} - < \bar{\rho}_m^n v_q^n >_{\theta-}]/\Delta z_j + [< \bar{\rho}_m^n r u_q^n >_{\lambda+} - < \bar{\rho}_m^n r u_q^n >_{\lambda-}]/r_i \Delta r_i\} \quad , \text{and} \tag{8}$$

$$\begin{aligned} e_{r,ij}^{n+1} = {} & \frac{1}{\bar{\rho}_{r,ij}^{n+1}} \{\bar{\rho}_{r,ij}^{n} e_{r,ij}^{n} - \frac{\Delta t}{\Delta z_j}[< \bar{\rho}_r^n v_q^n >_{\theta+} < e_r^n >_{\theta+} - < \bar{\rho}_r^n v_q^n >_{\theta-} < e_r^n >_{\theta-}] \\ & - \frac{\Delta t}{r_i \Delta r_i}[< \bar{\rho}_r^n r u_q^n >_{\lambda+} < e_r^n >_{\lambda+} - < \bar{\rho}_r^n r u_q^n >_{\lambda-} < e_r^n >_{\lambda-}] - p_{ij}^n (\epsilon_{r,ij}^{n+1} - \epsilon_{r,ij}^{n}) \\ & - \Delta t\, p_{ij}^n \left[\frac{< \epsilon_r^n r u_q^n >_{\lambda+} - < \epsilon_r^n r u_q^n >_{\lambda-}}{r_i \Delta r_i} + \frac{< \epsilon_r^n v_q^n >_{\theta+} - < \epsilon_r^n v_q^n >_{\theta-}}{\Delta z_j}\right]\} \quad . \end{aligned} \tag{9}$$

where $\lambda- = i-\frac{1}{2},j$, $\lambda+ = i+\frac{1}{2},j$, $\theta- = i,j-\frac{1}{2}$, and $\theta+ = i,j+\frac{1}{2}$.

In Eqs. (8) and (9), the n superscript refers to conditions at the end of Step 1 except for the pressure, which is not updated by Step 1. The axial and radial velocity components are denoted by v and u, respectively. The < > notation is described in Sec. IV.C. The estimated end-of-time-step volume fractions in Eq. (9) come from the smear densities calculated in Eq. (8). After evaluating Eqs. (8) and (9), the EOS is inverted to obtain temperatures consistent with the new densities and energies. Finally, Step 2 uses the momentum equations to calculate new velocities and velocity derivatives with respect to pressure. This operation is described in Sec. IV.B.

C. Step 3, Perform Iteration for Velocities and Consistent EOS Pressures

The anticipation of relatively quiescent problems in situations where the environment may have a high sonic velocity, for example, a pool, leads to the desire to calculate sonic wave progagation implicitly. The approach used in AFDM to accomplish this objective is semi-implicit differencing.[3] In the AFDM version of this approach, velocities are to be computed with EOS consistent pressures, with only selected (sensitive) variables or relationships being allowed to change from the Step 2 estimates. Besides the cell pressure itself, the sensitive variables (relationships) chosen are those describing each momentum density and the pressure-volume work term affecting the vapor internal energy. The error in pressure is given by

$$\epsilon_{ij} = f(\alpha_{5,ij}, \tilde{\rho}^{n+1}_{2,ij}, \ldots, \tilde{\rho}^{n+1}_{7,ij}, T^{n+1}_{2,ij}, \ldots, T^{n+1}_{5,ij}) - \tilde{p}^{n+1}_{ij} \quad . \tag{10}$$

The error in the conservation equations for the densities can be expressed by

$$D_{q,ij} = [\tilde{\rho}^{n+1}_{q,ij} - \bar{\rho}^{n}_{q,ij}]/\Delta t + [< \bar{\rho}^{n}_{q} \tilde{v}^{n+1}_{q} >_{\theta+} - < \bar{\rho}^{n}_{q} \tilde{v}^{n+1}_{q} >_{\theta-}]/\Delta z_j$$
$$+ [< \bar{\rho}^{n}_{q} r \tilde{u}^{n+1}_{q} >_{\lambda+} - < \bar{\rho}^{n}_{q} r \tilde{u}^{n+1}_{q} >_{\lambda-}]/r_i \Delta r_i \quad . \tag{11}$$

Within a momentum field, component density ratios are presumed to be constant during Step 3. The work term updates the vapor internal energy through the expression

$$D_{e_{G,ij}} = [(\tilde{\rho}^{n+1}_{G,ij})_o \tilde{e}^{n+1}_{G,ij} - \bar{\rho}^{n}_{G,ij} e^{n}_{G,ij}]/\Delta t + CE/\Delta t + \frac{\tilde{p}^{n+1}_{ij}}{\Delta t}(\tilde{\alpha}^{n+1}_{G,ij} - \alpha^{n}_{G,ij})$$
$$+ \tilde{p}^{n+1}_{ij} \frac{1}{\Delta z_j}[< e^{n} \tilde{v}^{n+1}_{G} >_{\theta+} - < e^{n} \tilde{v}^{n+1}_{G} >_{\theta-}]$$
$$+ \tilde{p}^{n+1}_{ij}[< e^{n}_{G} r \tilde{u}^{n+1}_{G} >_{\lambda+} - < e^{n}_{G} r \tilde{u}^{n+1}_{G} >_{\lambda-}]/r_i \Delta r_i \quad , \tag{12}$$

where the terms involving < e > have been collected into a convective term called CE that remains unchanged from Eq. (9) and the "o" subscript refers to densities from Eq. (8). These errors are to approach zero. This is accomplished by a multivariate Newton-Raphson procedure. In this procedure, the initial step is to expand the errors given by Eqs. (10)-(12) in a Taylor series. For example, the expansion for the mass conservation relationships, $D_{q,ij}$, is

$$D_{q,ij} + \frac{\partial D_{q,ij}}{\partial \tilde{\rho}_{q,ij}} \Delta \tilde{\rho}_{q,ij} + \frac{\partial D_{q,ij}}{\partial p_{ij}} \Delta p_{ij} + \frac{\partial D_{q,ij}}{\partial p_{i+1,j}} \Delta p_{i+1,j}$$
$$+ \frac{\partial D_{q,ij}}{\partial p_{i-1,j}} \Delta p_{i-1,j} + \frac{\partial D_{q,ij}}{\partial p_{i,j+1}} \Delta p_{i,j+1} + \frac{\partial D_{q,ij}}{\partial p_{i,j-1}} \Delta p_{i,j-1} = 0 \quad . \tag{13}$$

The derivatives in Eq. (13) can be evaluated using the velocity derivatives with respect to pressure calculated in Step 2. In this expansion, the change in the vapor

internal energy is expressed in terms of the independent EOS variables, the densities, and the temperatures. Ancillary expressions also are included so that density changes will modify the particle and liquid temperatures while holding the particle and liquid internal energies constant at the Step 2 values. After some algebra, the equations expressing Taylor series expansions can be written in a matrix form as

$$\underline{A}_{ij}\Delta\vec{x}_{ij} = -\vec{B}_{1ij}\Delta p_{i-1,j} - \vec{B}_{2ij}\Delta p_{i+1,j} - \vec{B}_{3ij}\Delta p_{i,j-1} - \vec{B}_{4ij}\Delta p_{i,j+1} - \vec{S}_{ij} \quad . \tag{14}$$

where the vector $\Delta\vec{x}_{ij}$ represents $(\Delta p_{ij}, \Delta\bar{\rho}_{q,ij}, \Delta T_{G,ij})^T$ .

Multiplication of Eq (14) by the first row of $A^{-1}(ij)$ gives n equations for the $\Delta p(ij)$, where n is the number of computational cells. When the change in pressure is known, the remaining cell-centered variables can be updated using the Taylor series expansions directly. The velocities are updated using the expressions for the velocity derivatives and the pressure changes. The multifield momentum equations are not solved here because of the lengthy computation involved and the stability problems discussed in Sec. IV.B. Determination of the velocities provides sufficient information for Eqs. (10)-(12) to be recalculated and another iteration started. Convergence is obtained when each of the variables in $\Delta\vec{x}$ is reduced below an input minimum.

D. Step 4: Update Variables for Consistent Convection

To obtain consistent convection of mass, momentum, and energy, the final updates are performed with convective terms using the velocities from Step 3. For example, the equations for mass conservation now become

$$\bar{\rho}_{m,ij}^{n+1} = \bar{\rho}_{m,ij}^{n} - \Delta t[[< \bar{\rho}_m^{n-n+1}\vec{v}_q^{n-n+1} >_{\theta+} - < \bar{\rho}_m^{-n-n+1}\vec{v}_q^{-n-n+1} >_{\theta-}]/\Delta z_j$$

$$+ [< \bar{\rho}_m^{n-n+1}ru_q^{n-n+1} >_{\lambda+} - < \bar{\rho}_m^{-n-n+1}ru_q^{-n-n+1} >_{\lambda-}]/r_i\Delta r_i) \quad . \tag{15}$$

A second optional operation in Step 4 is the inclusion of interfacial heating terms of the form $K(qq')|\vec{v}(q) - \vec{v}(q')|^2$ and $K(qS)|\vec{v}(q)|^2$ in the energy equations. Although these terms are desirable for complete energy conservation, it is believed they will not change results for LMFBR HCDA calculations significantly. If they do prove to be important, conceptually they should be included in the Step 1 vaporization, melting, and heat transfer models because of the origin of heating in the boundary layer. The inclusion in Step 4 is a computational convenience because of the presence of a consistent momentum equation.

The final operation of Step 4 is the convection of interfacial area a between continuous and discontinuous material components using the subscripts i and k, respectively, for the cell under investigation. The differential equation is adopted from Ishii,[4] and the initial AFDM approach is to use this equation in the form

$$\frac{\partial a_{i,k}}{\partial t} + \nabla\cdot(a_q\vec{v}_q) = S_{i,k} \quad . \tag{16}$$

The source terms in Eq. (16) are evaluated in Step 1. The q subscript in the convective term means that the interfacial area is convected with the velocity of the discontinuous phase. The exception is when a topology shift occurs between the cell under investigation and its neighboring cells. In this case, q refers to component i in the neighboring cell, and a(q) is given by a(i,continuous phase) of the neighboring cell. The differencing of Eq (16) then proceeds similarly to the other differential equations. This completes an outline of the AFDM algorithm.

## IV. AFDM COMPUTATIONAL FEATURES

### A. Virtual Mass

Before the momentum equation solution can be discussed, the virtual mass term in Eq. (2) must be defined. This term arises when a dispersed phase is accelerated in a multiphase medium. The acceleration gives rise to an additional force because a part of the neighboring fluid also must be accelerated. A general formulation of the virtual mass term for two-phase flow based on the objectivity principle was developed by Drew.[5] The analysis shows that the virtual mass force between a continuous phase, i, and a discontinuous phase, k, has the form

$$\vec{F}_{ik} = \alpha_k \rho_i C_k \left[ \left( \frac{\partial}{\partial t} + \vec{v}_i \cdot \nabla \right) \vec{v}_k - \left( \frac{\partial}{\partial t} + \vec{v}_k \cdot \nabla \right) \vec{v}_i + (1 - \lambda)(\vec{v}_k - \vec{v}_i) \cdot \nabla (\vec{v}_i - \vec{v}_k) \right] \quad . \tag{17}$$

where C(k) is called the virtual mass coefficient and $\lambda$ is mainly a function of the volume fraction of the discontinuous phase.

Besides the above rationale, the use of virtual mass terms can remove the complex characteristics that otherwise exist with the use of one averaged cell pressure in the momentum equations. The numerical stability of a multiphase calculation may be improved.

Because of the uncertainties that still exist, the approach adopted was to include only those virtual mass terms whose anticipated or observed effects appear cost effective to retain. Four considerations were used to reduce Eq. (17) to fit Eq. (2). First, only those virtual mass terms that deal with the interaction of a discontinuous vapor with a continuous liquid were retained. If vapor is continuous, the density coefficient in Eq. (17) is small. For liquid-liquid interactions, the standard drag coefficient is large, and terms based on acceleration have little effect. Second, Eq. (17) was programmed in a trial two-phase, one-dimensional algorithm to investigate its effects on calculations. We found that the value of $\lambda$ best promoting stability was problem dependent. A general constant value could not be selected. This led to the formulation of other arguments, resulting in the conclusion to drop the convective terms from Eq. (17), leaving only the inertial terms. Third, momentum feedback from the discontinuous vapor somehow must be apportioned to the two liquid fields. For convenience, this division was performed based on the liquid volume fractions present. Fourth, the virtual mass coefficient was defined based on formulas adapted from Ishii.[6] The virtual mass terms in Eq. (2) then have the form

$$\vec{VM}_1 = -\alpha_{1,\text{eff}} \vec{VM}_6 \quad , \quad \vec{VM}_2 = -\alpha_{2,\text{eff}} \vec{VM}_6 \quad , \text{ and}$$

$$\vec{VM}_6 = -\alpha_6 \rho_{L,\text{eff}} C_6 \left[ \frac{\partial \vec{v}_6}{\partial t} - \alpha_{1,\text{eff}} \frac{\partial \vec{v}_1}{\partial t} - \alpha_{2,\text{eff}} \frac{\partial \vec{v}_2}{\partial t} \right] \quad . \tag{18}$$

where the numeric subscripts stand for liquid momentum fields and the effective liquid density is a volume-averaged quantity. The virtual mass term as defined above is particularly useful in stabilizing the higher-order differencing format when describing churn-turbulent flow.

### B. Three Velocity Fields

To provide a better representation of fuel-coolant interactions, pool stratification, and other HCDA phenomena, the AFDM is written in terms of three velocity fields. The approach can be extrapolated readily to more velocity fields if the momentum exchange relationships can be defined. The key difficulty is solving the momentum equations. The approach used is a modification of that done previously.[1] The finite-difference form of the momentum equations is straightforward except for the convective term and the treatment of the interfield drag terms. (Unfortunately, space does not permit a full discussion of the convective terms.) As an example, in Step 4 the axial convective term (ignoring the q subscript) is given by

$$\frac{1}{r}\frac{\partial}{\partial r}(\bar{\rho}vru) + \frac{\partial}{\partial z}(\bar{\rho}v^2) = \frac{1}{r_i \Delta r_i}[< \bar{\rho}^n ru^{n+1} >_{i+\frac{1}{2},j+\frac{1}{2}} < v^n >_{i+\frac{1}{2},j+\frac{1}{2}}$$

$$- < \bar{\rho}^n ru^{n+1} >_{i-\frac{1}{2},j+\frac{1}{2}} < v^n >_{i-\frac{1}{2},j+\frac{1}{2}}] + [< \bar{\rho}^n v^{n+1} >_{i,j+1} < v^n >_{i,j+1}$$

$$- < \bar{\rho}^n v^{n+1} >_{ij} < v^n >_{ij}]/\Delta z_{j+\frac{1}{2}} \quad . \tag{19}$$

with the < > terms discussed in Sec. IV.C. The initial approach for the drag terms was to use end-of-time-step (ETS) velocities wherever a velocity difference appeared, including any velocity differences used in the model for K(q,q'). The difficulty with this approach was that oscillations occurred in attempting to iterate as a function of pressure drop. An example is shown in Fig. I. The main curve is an example solution to the AFDM vapor momentum equation as a function of the pressure difference between two cells for highly dispersed flow. Starting at point A, an extrapolation using the velocity derivative as a function of pressure is along the line A-B. An evaluation of the velocity with a pressure drop corresponding to B gives the point C. The velocity derivative then moves along line C-D, and a function evaluation at point D gives a velocity very close to point A. The solution to this problem was to adopt the definition

$$\vec{v}_{q',\xi} - \vec{v}_{q,\xi} = (1-\omega)\vec{v}^{n}_{q',\xi} + \omega\vec{v}^{n+1}_{q',\xi} - (1-\omega)\vec{v}^{n}_{q,\xi} - \omega\vec{v}^{n+1}_{q,\xi} \quad . \tag{20}$$

where $\xi$ can represent either $\theta+$ or $\lambda+$, in other words, an axial or radial coordinate. The quantity $\omega$ is set to one-half in Step 2 and to unity in Step 4. The derivatives of the velocity with respect to pressure for Step 3 are obtained from differentiating the finite-difference form of the momentum equation in Step 2. This procedure partially updates the velocities in the desired direction in Steps 2 and 3 and then eliminates undesired previous time-step effects from the interfield drag in Step 4. For example, if a flow-regime shift occurs, using ETS velocities in the drag eliminates a time-step size dependence in the adjustment to a new flow regime.

C. Higher Order Differencing

In assessing the recriticality of a disrupted LMFBR core, a key parameter is how much fuel remains in the core vicinity. The numerical diffusion associated with first-order accurate donor cell differencing can be quite nonconservative in performing this estimate. When performing postdisassembly expansions, excessive numerical diffusion also can be considered as causing energy smearing and a reduction in the work performed. In AFDM, a higher order differencing approach has been adopted from van Leer.[7] The idea is to define both the magnitude and slope of a variable in a donor cell. The time-step size furnishes an integration distance for determining convection. Limiters then are used to stop oscillations and ensure that the scheme remains positive definite. As an example, the < > quantities in the axial direction are defined by

$$< \bar{\rho}v >_{\theta+} = [\bar{\rho}_{ij} + \frac{\Delta z_j}{2}(\frac{\partial\bar{\rho}}{\partial z})_{ij}]v_{\theta+} - \tfrac{1}{2}(\frac{\partial\bar{\rho}}{\partial z})_{ij} v^2_{\theta+}\Delta t \quad , \; v_{\theta+} > 0 \quad , \text{ and}$$

$$< \bar{\rho}v >_{\theta+} = [\bar{\rho}_{i,j+1} - \frac{\Delta z_{j+1}}{2}(\frac{\partial\bar{\rho}}{\partial z})_{i,j+1}]v_{\theta+} - \tfrac{1}{2}(\frac{\partial\bar{\rho}}{\partial z})_{i,j+1} v^2_{\theta+}\Delta t \quad , \; v_{\theta+} < 0 \quad . \tag{21}$$

In Eq. (21) the slope of the density is given by

$$(\frac{\partial\bar{\rho}}{\partial z}) = \text{sign}(\frac{\partial\bar{\rho}}{\partial z})\,\min[|(\frac{\partial\bar{\rho}}{\partial z})|, |(\frac{\partial\bar{\rho}}{\partial z})|, |(\frac{\partial\bar{\rho}}{\partial z})|]$$

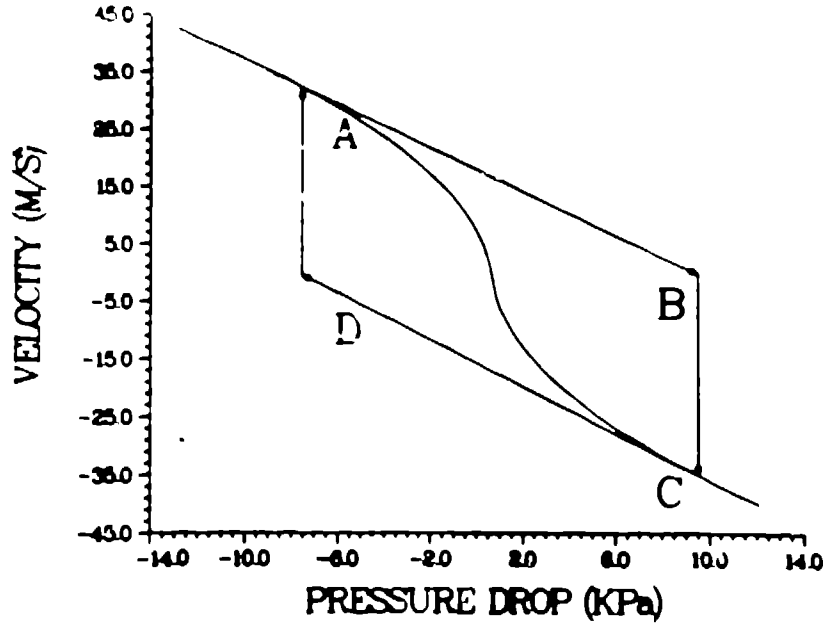


Fig. 1.

Vapor velocities at a 0.98 vapor volume fraction.

$$(\frac{\partial\bar{\rho}}{\partial z})_{1j} = 0 \text{ if } \text{sign}(\frac{\partial\bar{\rho}}{\partial z})_{2,1j} \neq \text{sign}(\frac{\partial\bar{\rho}}{\partial z})_{3,1j} \text{ , where}$$

$$(\frac{\partial\bar{\rho}}{\partial z})_{1,1j} = \frac{\bar{\rho}_{1,j+1} - \bar{\rho}_{1j}}{\Delta z_{j+1} + \Delta z_j} + \frac{\bar{\rho}_{1j} - \bar{\rho}_{1,j-1}}{\Delta z_j + \Delta z_{j-1}} \text{ ,}$$

$$(\frac{\partial\bar{\rho}}{\partial z})_{2,1j} = \frac{2(\bar{\rho}_{1,j+1} - \bar{\rho}_{1j})}{\Delta z_j} \text{ , and } (\frac{\partial\bar{\rho}}{\partial z})_{3,1j} = \frac{2(\bar{\rho}_{1j} - \bar{\rho}_{1,j-1})}{\Delta z_j} \text{ .}$$

Similar definitions exist for the radial direction, but the slope of a convected quantity is based on the area, not the radial coordinate alone.

The energy terms $< e >$ are evaluated by averaging over the volume from which the corresponding mass was taken using an energy shape defined in a manner similar to the density. This results in an equation similar to that of Eq. (21) but with one velocity factor removed. Equation (21) is volume-averaged over the two relevant cells to obtain the momentum terms in Eq. (19). The $< v >$ term in Eq. (19) is evaluated by integrating an assumed velocity shape over the volume corresponding to the transported momentum. This is implemented by basing the limits of integration on a velocity defined by dividing the momentum flux by an appropriately volumetrically averaged density. The original van Leer algorithm is second order accurate in space except where the limiters apply and when a nonuniform mesh is selected. In AFDM, the staggered mesh, which was chosen to help pressure-velocity calculative stability, makes the accuracy in momentum transport hard to evaluate. Consequently, the slightly ambiguous term, higher order differencing was selected to describe this approach, and the criterion for its evaluation is performance. The scheme does appear to work reasonably well. There is a penalty incurred from the lengthened formulas and extra iterations required for convergence in Step 3, but it appears acceptable in the cases investigated so far. An example of modification in results obtained with higher order differencing is given in Sec. V.

D. Treatment of Interfacial Area

The interfacial areas between components must be known to assess Step 1 intracell transfers. AFDM interfacial areas at present are defined for unrestricted flow only. Velocity and concentration profiles imposed by solid structures are presumed not to influence the flow regime that is present. A cell is initialized by (a) selecting the topology based on volume fractions and relative velocities and (b) obtaining the convective interfacial areas between continuous and discontinuous components from Eq. (16). Operation 3 in Step 1 modifies these areas with a source term. This reflects the change of surface area within a given cell as a result of several physical processes such as nucleation, dynamic forces, turbulence, coalescence, and surface tension forces. In general, models for the source term are simple. For example, dynamic forces modify the radii of bubbles/droplets by a first-order differential equation expressing the idea that the equilibrium Weber number can be approached using a relaxation-time model.

When the continuous liquid, the continuous phase, and the source term have been assessed, the interfacial areas of the discontinuous components can be updated. However, they share parts of their surfaces with coexisting discontinuous components or with the solid structure. Therefore, several contact criteria are specified to define the surface subdivision, such as the contact to the solid structure, the interface between Liquid 1 and its solid phase, the contact of the vapor and two liquid components at zero velocity through contact angles, the contact of two discontinuous components at finite velocity differences, and the combination of the latter two processes. Finally, after the results of the AFDM heat and mass transfer models are known, the interfacial areas are updated based on the mass transfer results, in preparation for the calculation of momentum convection and convection of interfacial area itself. Figures II and III show two topologies with all components present in a cell.

In Fig. II, vapor is the continuous phase. The prevailing droplet flow consists of two types of droplets. One droplet consists of the solid and liquid phase of component 1, and the other contains the single component L2. The broken-line circles next to the L2 droplet indicate that the contact to the P/L1 droplet may be a function of the velocity difference by using a collision frequency model. In Fig. III, Liquid 1 is continuous. Therefore, its solid phase (represented by the

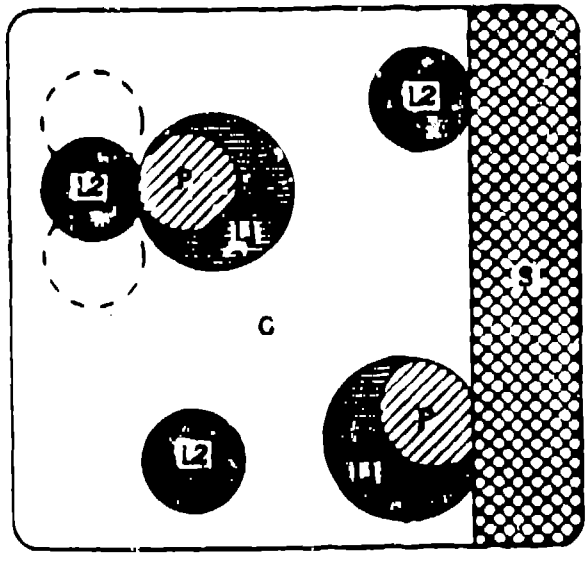


Fig. II.
Topology with dispersed flow.

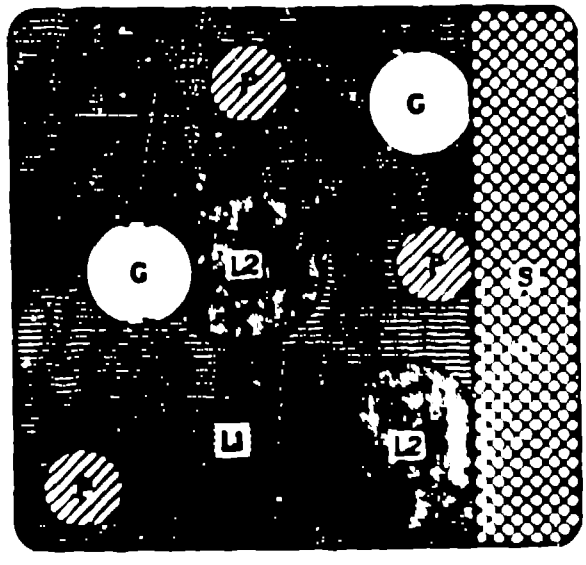


Fig. III.
Topology with bubbly flow.

particles, P) is embedded totally in the liquid, except for the contact to the solid structure. Ll and P have the same velocity. Again, the contact between the other discontinuous phases is defined by contact angle criteria and the velocity difference.

E. AFDM Heat and Mass Transfer

A simple heat and mass transfer model is being implemented in the first version of AFDM. The phase transition processes included are melting and freezing of fuel and evaporation and condensation of fuel and steel. The calculative model is similar to the SIMMER-II description of heat and mass transfer and computes mass transfer rates from heat transfer to the respective interfacial areas.[2] Heat transfer itself is calculated by using appropriate heat transfer coefficients for the various possible configurations and the temperature differences between the components and phases. (The gas phase, which consists of totally mixed components, is characterized by one energy and temperature.)

A more sophisticated phase-transition model, which tracks physical processes more accurately, also is being developed for the AFDM. This model is characterized by a separate treatment of mass transfer. Evaporation and condensation is represented by multicomponent and diffusion processes in the vapor phase. The diffusion equation used is

$$N_i = c_t \sum_{j,k} B_{ij} D_{jk} \Delta y_k / \ell \quad . \tag{22}$$

In this equation, i, j, and k are component indices, and the finite concentration differences $\Delta y(k)$ are divided by the boundary layer thickness $\ell$. The D(j,k) denote a 2 x 2 matrix of diffusion coefficients for averaged values of the concentrations, c(t) is the total molar density of the gas mixture, and B(i,j) is the "bootstrap" matrix. When the third component is not condensible (as in the AFDM), B(i,j) is given by

$$B_{ij} = \delta_{ij} + y_i/y_3 \quad . \tag{23}$$

where $\delta_{ij}$ is the Kronecker delta function. Interfacial temperatures (denoted by I) for evaporation and condensation are determined by interphase heat transport equations of the form

$$h_{I,Ll}(T^I_{Ll} - T_{Ll}) + h^*_{G,Ll}(T^I_{Ll} - T_G) = \sum_i N_i M_i \Delta h_{Li,eff} \quad .$$

Here h(I,Ll) is the heat transfer coefficient from the gas/liquid interface into the liquid (Ll) phase, h*(G,Ll) is the mass-flux-corrected heat transfer coefficient from the gas/liquid interface into the multicomponent gas phase, M(i) is the molecular weight, and the effective enthalpy of vaporization is evaluated to insure conservation of energy. Two problems have to be resolved to find the concentration gradients in the boundary layer: (1) the concentration at the interface and (2) the size of the concentration boundary layer. Problem (1) is solved by using equilibrium assumptions and the EOS at the interface. The pressure at the interface is presumed to be the AFDM cell pressure. Problem (2) is solved by using mass-transfer correlations as given in the chemical literature or from analogies between heat and mass transfer. (The latter method has the advantage of guaranteeing the consistency in heat and mass transfer calculations automatically.)

F. Equation of State

The multicomponent EOS package in the AFDM is based on the SESAME[8] philosophy of EOS evaluation. The SESAME EOS system is a standardized, computer-based library of tables of thermodynamic properties and FORTRAN subroutines. The data library currently contains information for roughly 70 materials. Using the SESAME system, pressures, internal energies, and free energies are available as a function of density and temperature. Associated partial derivatives, saturation properties, and

inverse EOS evaluations also are available. The SESAME software contains vectorized routines[9] to interpolate the library data tables and utilities[10] to update existing data libraries with new material flexibility and data accuracy improvement capabilities.

The set of independent variables with which the AFDM solution algorithm proceeds is composed of macroscopic densities and temperatures ($\bar{\rho}$ and T). An independent variable vector for the AFDM algorithm can be written as

$$\vec{x}_F = (\bar{\rho}_p, \bar{\rho}_{L1}, \bar{\rho}_{L2}, \bar{\rho}_{G1}, \bar{\rho}_{G2}, \bar{\rho}_{G3}, T_p, T_{L1}, T_{L2}, T_G)^T \quad . \tag{25}$$

This vector represents the information normally available for EOS queries.

The main complexity in the implementation of the SESAME EOS is in the transformation of the macroscopic density information appearing in $\vec{x}(F)$ to microscopic density information needed for EOS evaluations. This is handled by assuming mechanical equilibrium (in pressure) between the various material components in a numerical cell and then proceeding in the following way. The ga microscopic densities first are defined as

$$\vec{\rho}_G = \vec{\bar{\rho}}_G / \max(\bar{\alpha}, \alpha_G) \quad , \tag{26}$$

where $\bar{\alpha} \equiv (1 - \alpha_S)\alpha_0$ , and (27)

$$\alpha_G \equiv 1 - \alpha_S - (1 - \alpha_0)(\alpha_{L1} + \alpha_{L2} + \alpha_p). \tag{28}$$

The quantity $\alpha_0$ is an input parameter representing a small amount of gas volume that is to be maintained even in single-phase liquid cells. The structure volume fraction $\alpha_S$ is considered a cell-dependent problem input parameter.

To complete the description of the gas micro-densities, physical volume fractions for the cell must be defined. Their definition uses saturated liquid densities that are determined from a statement of mechanical equilibrium between all the components, or

$$P_G(\vec{\rho}_G, T_G) = P_{L1}(\rho_{sL1}, T_{L1}) = P_{L2}(\rho_{sL2}, T_{L2}) = P_p(\rho_{sp}, T_p) \quad , \tag{29}$$

where the microscopic saturated densities appearing in Eq. (29) are determined with the volume fractions used to define $\alpha_G$ in Eq. (28) by the expression

$$\rho_{sm} = \bar{\rho}_m / \alpha_m \quad , \quad m = p, L1, \text{ and } L2 \tag{30}$$

Assuming that the EOS provides all the pressures appearing in Eq. (29) and given $\vec{x}(F)$, then the system of Eqs. (26)-(30) representing 10 equations contains 10 unknowns ($\rho_{G1}, \rho_{G2}, \rho_{G3}, \rho_{sL1}, \rho_{sL2}, \rho_{sp}, \alpha_G, \alpha_{L1}, \alpha_{L2}, \alpha_p$) and therefore can be solved to determine all the $\alpha$'s. With algebraic substitution this system can be reduced to three equations containing the three liquid-field $\alpha$'s, and then solved numerically with a Newton-Raphson iteration

In single-phase liquid cells, a similar statement of mechanical equilibrium is used to define the compressed liquid and particle volume fractions. A complete description of the EOS package and its complexities (such as material mixture rules, the total pressure model, partial derivatives, and the use of the spinodal dome) is in preparation

8. Vectorization

An attempt is being made in the programming of AFDM to obtain complete vectorization of all numerical calculations This can be accomplished by (1) memory management, (2) elimination of nested loops, (3) removing calls to subroutines and

functions from loops doing numerical calculations, and (4) removing conditional statements from loops doing numerical calculations.

The conservation of memory is considered only if vectorization is not inhibited. With the memory size of current vector computers, memory should not be a problem. The parameters that determine the mesh size should be selected so that memory conflicts are eliminated. Each mesh variable is assigned a contiguous block of memory to optimize the fetching/storing of the variable.

"DO" loops are nested only when they do not affect the optimization of vectorization. If nested "DO" loops must be used, the "DO" loop with the largest range of indices must be the innermost loop. Calls to subroutines are not allowed in "DO" loops because they inhibit vectorization. To achieve this, each call to a subroutine must do its calculation over the range of the "DO" loops.

Conditional statements can be eliminated by (1) gather/scatter and (2) vector merge techniques. For the gather/scatter technique, tables of different classes of variable are set up. Using these tables the calculation for each class of variable is done by vectorized loops. A truth vector is generated for the vector merge technique. The truth vector selects one of several variables to calculate the value of a third variable in a vectorized loop.

The AFDM program has been developed on a Cray 1 computer. As a rule of thumb on the CRAY-1, the advantage of a vectorized program over an optimized nonvectorized program is about a factor of 4.

## V. AFDM Status

Initially, some of the ideas to be used in the AFDM algorithm (the SESAME EOS, the higher order differencing, the multiple flow regimes, the virtual mass treatment, and the pressure iteration itself) were investigated with a one-dimensional, two-phase code. Next, a basic two-dimensional AFDM algorithm as described in Sec. III was programmed and is operational. The more sophisticated models are currently in the programming/debugging process. It is premature at this time to report a significant LMFBR HCDA calculation. Completion of this phase of the AFDM project with the models as defined here is scheduled for October 1987.

Relatively simple checkout calculations are being performed at this stage. As an example, a comparison has been done with an isothermal two-liquid experiment performed at Kernforschungszentrum, Karlsruhe. In this experiment, tetralin (simulating uranium dioxide) is mixed with ammonia (simulating steel). The initial experimental configuration is shown in Fig. IV. The figure dimensions are in millimeters, and the box is 51.5 mm thick. The experiment is performed by withdrawing a cylinder and releasing the tetralin. To obtain a calculation that can be compared with this experiment, three dimensions are desirable, but planar geometry can be used for a first approximation. The AFDM currently is programmed in r-z geometry. Although a planar option is planned, it does not presently exist. To partially simulate planar geometry, the calculation was performed in annular geometry with a large center (100-m) node of solid structure. With the remaining radial nodes being ~5.5 mm, the cylindrical aspect of the calculation is eliminated. Because the models discussed in Sec. IV.D still are being implemented, these calculations were performed with constant radii (for drag) of 0.5 mm for tetralin and 1 mm for ammonia. The calculative representation of the configuration is shown in Fig. V. Each contour represents a 10% change in volume fraction. Figures VI and VII give the calculative results using both the donor cell and the higher order differencing approaches. Figure VIII gives an outline of an experimental tetralin profile as inferred from the high-speed movie for comparison. Although caveats exist, the comparison is reasonable. Higher order differencing does produce a reduction in numerical dissipation and an initial reduction in smearing. Both the experiment and the calculation slosh the tetralin up the sides to approach/touch the upper ammonia surface. However, the calculation is incorrectly trapping ammonia in the right corner at 300 ms. The counterflow of the escaping ammonia causes turbulence that lasts much

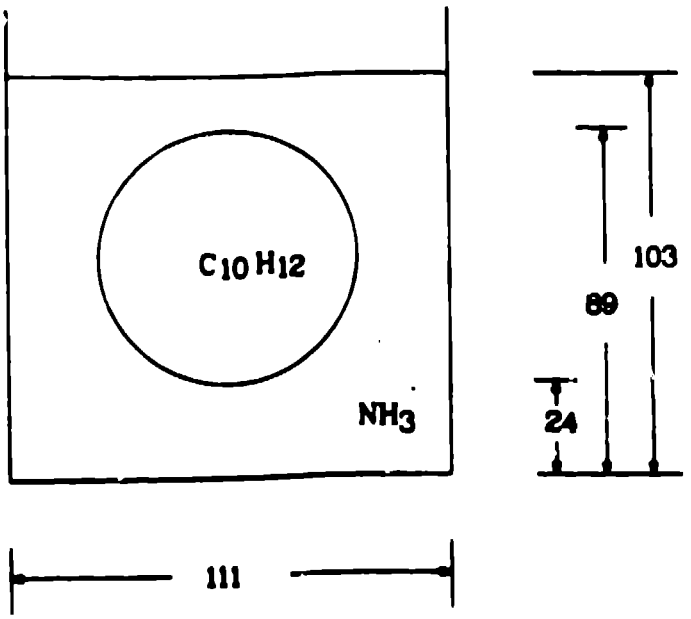


Fig. IV.
Experimental simulation.

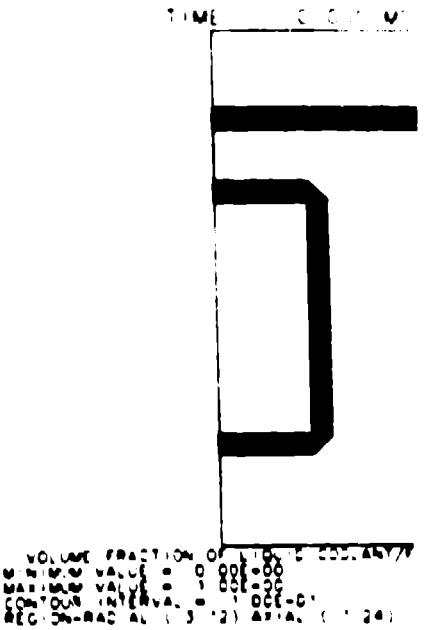

Fig. V.
Calculational simulation.

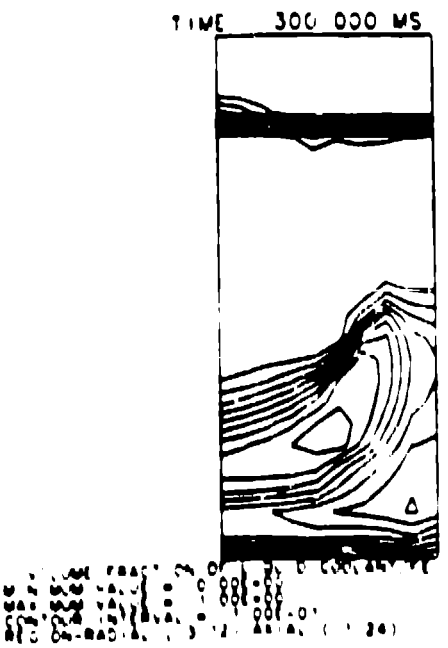


(a)

(b)

Fig. VI.
First-order donor cell results.

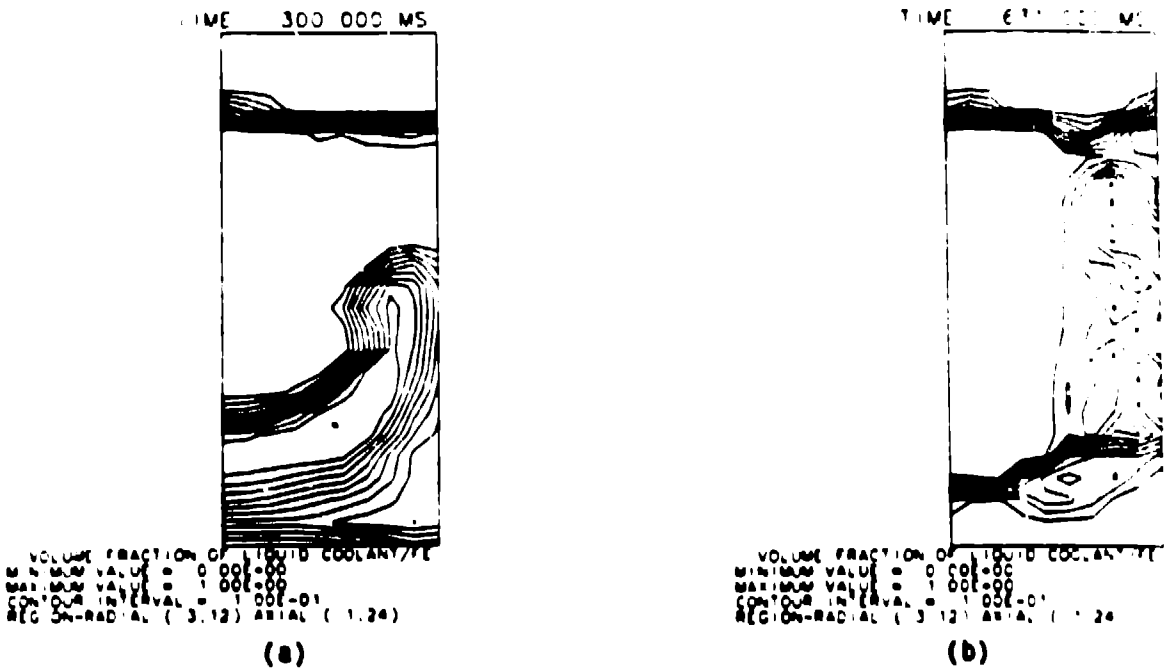


Fig. VII.
Higer-order differencing.

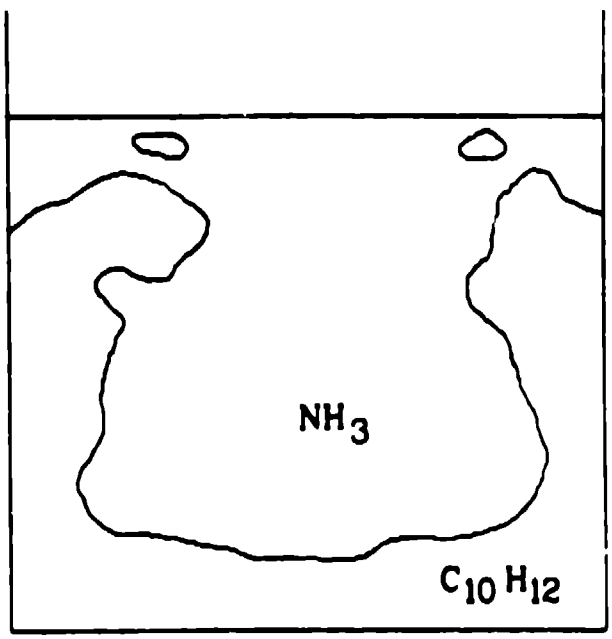


Fig. VIII.
Experimental tetralin profile at 631 ms.

longer with the higher order differencing format. Investigation with the more sophisticated interfacial area model is planned. Computational "bugs" almost certainly exist with a computer code at the AFDM's developmental stage. The experimental

results are less than ideal because of tetralin splashing on the front viewing window and because of turbulence and loss of ammonia caused by withdrawing the cylinder. The experiment is being rerun to check reproducibility and to eliminate some ammonia vapor bubbles caused by radiation from the outside environment.

To summarize, progress is being made in the investigation of techniques that will reduce LMFBR HCDA calculative uncertainties. It is premature at this time to judge the ultimate usefulness of the more complex innovations. Changes in the algorithm described here can be anticipated. However, compared with SIMMER-II,[2] sufficient progress has been made to conclude that, with further development, significant improvements are possible in reliably calculating the progression of severe accidents.

REFERENCES


1. W. R. Bohl, "A Calculational Advance in the Modeling of Fuel-Coolant Interactions," in Proc. LMFBR Safety Topical Meeting (Lyon, France, 1982), p. III-557.

2. W. R. Bohl and L. B. Luck, "SIMMER-II: A Computer Program for LMFBR Disrupted Core Analysis," Los Alamos National Laboratory report, LA-7515-M, NUREG/CR-0453, Rev. 2 (in preparation).

3. D. R. Liles and W. H. Reed, "A Semi- Implicit Method for Two-Phase Fluid Dynamics," J. Comp. Phys., 26, 77 (1978).

4. M. Ishii, Thermo-Fluid Dynamic Theory of Two-phase Flow (Collection de la Direction des Etudes et Recherches D'Electricite de France, Eyrolles, 1975).

5. D. Drew, L. Cheng, and R. T. Lahey, Jr., "The Analysis of Virtual Mass Effects in Two-Phase Flow," Int. J. Multiphase Flow, 5, 233-242 (1979).

6. M. Ishii and K. Mishima, "Two-Fluid Model and Hydrodynamic Constitutive Relations," Nuc. Engrg. Des., 82, 107-126 (1984).

7. Bram van Leer, "Towards the Ultimate Conservative Difference Scheme. IV. A New Approach to Numerical Convection," J. Comp. Phys., 23, 276-299 (1977).

8. K. S. Holian, Editor, "T-4 Handbook of Material Properties Data Bases, Vol. Ic: Equations of State," Los Alamos National Laboratory report LA-10160-MS (November 1984).

9. Charles W. Cranfill, "EOSPAC: A Subroutine Package for Accessing the Los Alamos Sesame EOS Data Library," Los Alamos National Laboratory report LA-9728-M (August 1983).

10. J. Abdallah, Jr., "User's Manual for GRIZZLY," Los Alamos National Laboratory report LA-10244-M (September 1984).

# Los Alamos

Los Alamos National Laboratory
Los Alamos, New Mexico 87545

## TECHNICAL INFORMATION RELEASE
**(Category I or II Unclassified Information Only)**

INSTRUCTIONS: Submit to OS-6 Classification Group with abstract or paper **before** presentation or submittal for publication.
APPROVAL: Division-level approval required on all abstracts and full papers. Abstract or summary is required and sufficient for approval of talk. Patentable matter should be discussed directly with Patent Law to avoid delays. LA-UR cover (Form 836) required on all copies of full papers. Allow one day for review.
PARTICULARS: *Publications*: Give details as to where article is to be submitted for publication. *Presentation*: Give details as to name/sponsor, place, and date of presentation.

COPIES REQUIRED BY CLASSIFICATION GROUP
One of this form
Two of abstract (cover optional)
Three of full paper (cover required)

LA-UR 86-4359

AUTHOR(S) (Full Name) Group or Affiliation

W(illiam) R. Bohl, Q-6
L(arry) B. Luck, Q-6
D(irk) Wilhelm, KfK
F(red) R. Parker, Q-6
J(ean) Berthier, CEA
P(aul) J. Maudlin, Q-6
P(hilipp) Schmuck, KfK
L(uc) Goutagny, CEA
S(hinichi) Ichikawa, FACOM-HITAC
H(isashi) Ninokata, PNC

AUTHOR(S) (Signature and Date)

Fam. P. Fred 21 Dec 86

Title of Article (In Caps) (Spell out all symbols)

COMPUTATIONAL METHODS OF THE ADVANCED FLUID DYNAMICS MODEL

☐ Abstract
☒ Full Paper
☐ Other

Intended For: ☐ Journal ☒ Proceedings ☒ Meeting ☐ Talk ☐ Other

Particulars: to be presented at the ANS International Meeting on Advances in Reactor Physics, Mathematics, and Computation, Paris, France, April 27-30, 1987

| Deadline Date | Group Office Telephone | Mail Stop |
|---|---|---|
| January 10, 1987 | 7-6231 | K557 |

| | |
|---|---|
| Category I<br>Program Code R282 | Division Leader(s) Signature and Date<br>William S. Hall 12/30/86 |
| Category II<br>Program Code | Division Leader(s) Signature and Date |

## CLASSIFICATION GROUP

| Date Received | DOE/NRC Category | Group/Author Notification Of Release |
|---|---|---|
| 12 31 86 | L 79p | Classified |

## PATENT LAW

| Patent Interest | Docket Number | Patent Law Reviewer and Date |
|---|---|---|
| ☐ Yes ☐ No | | |

COMMENTS: Cannes 12/31/86
Nice-Acropolis, Palais Acropolis

Rev. 5 RS

Form available from Classification Group